

# Unprecedented evidence for overshooting convection hydrating the tropical stratosphere

T. Corti,<sup>1</sup> B.P. Luo,<sup>1</sup> M. de Reus,<sup>2</sup> D. Brunner,<sup>3</sup> F. Cairo,<sup>4</sup> M.J. Mahoney<sup>5</sup> G. Martucci,<sup>6</sup> R. Matthey,<sup>6</sup> V. Mitev,<sup>6</sup> F. H. dos Santos,<sup>7</sup> C. Schiller,<sup>7</sup> G. Shur,<sup>8</sup> N.M. Sitnikov,<sup>8</sup> N. Spelten,<sup>7</sup> H.J. Vössing,<sup>2,9</sup> S. Borrmann,<sup>2,9</sup> and T. Peter<sup>1</sup>

---

T. Corti, Institute for Atmospheric and Climate Science, Universitätstrasse 16, CH-8092 Zurich, Switzerland. (tcorti@env.ethz.ch)

<sup>1</sup>Institute for Atmospheric and Climate Science, Swiss Federal Institute of Technology (ETH), Zurich, Switzerland

<sup>2</sup>Institute for Atmospheric Physics, Johannes-Gutenberg-University, Mainz, Germany

<sup>3</sup>Laboratory for Air Pollution and Environmental Technology, Empa, Dübendorf, Switzerland

<sup>4</sup>Istituto di Scienze dell'Atmosfera e del Clima, Consiglio Nazionale delle Ricerche, Rome, Italy

We report on in-situ and remote sensing measurements of ice particles in the tropical stratosphere found during the Geophysica campaigns TROC-CINOX and SCOUT-O3. We show that deep convective systems penetrate the stratosphere and deposit ice particles at altitudes reaching 420 K potential temperature. These convective events have a hydrating effect on the lower tropical stratosphere, whereas there were no signs of convectively induced dehydration.

---

<sup>5</sup>Jet Propulsion Laboratory, California

Institute of Technology, Pasadena, CA, USA

<sup>6</sup>Observatoire Cantonal de Neuchatel,

Neuchatel, Switzerland

<sup>7</sup>Institute for Stratospheric Research,

Forschungszentrum Jlich, Jlich, Germany

<sup>8</sup>Central Aerological Observatory,

Moscow, Russia

<sup>9</sup>Particle Chemistry Department,

Max-Planck-Institute for Chemistry, Mainz,

Germany

## 1. Introduction

Air enters the stratosphere in the tropics [*Brewer, 1949*], where it is transported from the upper troposphere across the tropopause situated at about 380 K potential temperature ( $\approx 17$  km) into the stratospheric overworld [*Holton et al., 1995*] and further toward higher latitudes in the Brewer-Dobson circulation. It is well known that moist boundary layer air is transported into the upper troposphere by deep convection with a main outflow region at about 13 km [*Folkens and Martin, 2005*]. How the air reaches the stratosphere is in contrast subject of ongoing debate. The way by which the rising air is dehydrated is closely linked to the transport mechanism of troposphere-to-stratosphere transport (TST) and equally uncertain.

Two classes of hypotheses have emerged to explain dehydration. “Cold trap dehydration” assumes a large-scale upwelling motion as main mechanism, involving quasi-horizontal transport through a “fountain” region over the maritime continent and Western Pacific [*Newell and Gould-Stewart, 1981; Holton and Gettelman, 2001*]. The air is thereby gradually dehydrated in cirrus clouds. This hypothesis is supported by the distribution of high cirrus clouds [e.g., *Wang et al., 1996*], the geographical and temporal distribution of water vapor [*Read et al., 2004*], trajectory studies [e.g., *Jensen and Pfister, 2004; Fueglistaler et al., 2004*] and radiative calculation [*Corti et al., 2006*].

The alternative hypothesis, “convective dehydration”, postulates that dehydration occurs mainly in very deep, overshooting convection [e.g., *Danielsen, 1982, 1993; Sherwood and Dessler, 2001*]. This mechanism invokes overshooting to lead to extremely dry air caused by the extremely low temperatures in cumulonimbus turrets. However, efficient

dehydration requires an air parcel to be exposed to these low temperatures for a sufficiently long time so that the ice particles have a chance to sediment out [*Holton and Gettelman, 2001*]. It is questionable whether convective overshoots satisfy this requirement. In contrast, model simulations suggest that overshooting convection has rather a hydrating than dehydrating effect [*Chaboureau et al., 2007*].

There are several reports on tropical deep convection reaching into the stratosphere [e.g., *Adler and Mack, 1986; Danielsen, 1993*] leaving open whether the air eventually mixed into the stratosphere or descended back into the troposphere. Conversely, of ice [*Kelly et al., 1993*] or other solid particles [*Nielsen et al., 2007*] above 380 K could not be linked unambiguously to convective overshoots.

The question whether overshooting convection leads to hydration or dehydration is basically still open. The present study reports on airborne in situ and remote observations of ice particles in the tropical stratosphere during two recent aircraft campaigns tackling two questions: Are the observed stratospheric ice particles the result of overshooting convection and mixing? And are they hydrating or dehydrating the stratosphere?

## 2. Instruments and Data

In 2005, two missions involving the high altitude research aircraft Geophysica aimed at shedding light on these questions: the Tropical Convection, Cirrus, and Nitrogen Oxides Experiment (TROCCINOX) in the State of Sao Paulo, Brazil in February 2005 and the Stratosphere-Climate Links with Emphasis on the Upper Troposphere and Lower Stratosphere (SCOUT-O3) tropical experiment in Darwin, Australia, in November/December 2005 [*Vaughan et al., 2007*]. We use measurements from various instruments operated on-

board the Russian high altitude research aircraft Geophysica [*Stefanutti et al.*, 1999]. Two instruments measure gas phase water and total water, the Fluorescent Airborne Stratospheric Hygrometer (FLASH) [*Sitnikov et al.*, 2007] and the Fast In situ Stratospheric Hygrometer (FISH) [*Zoger et al.*, 1999], respectively. Both instruments use the Lyman  $\alpha$  fluorescence technique. The ice water content was calculated from the difference between these two instruments taking particle sampling enhancement into account. Cloud free periods were determined as the subset of measurements with water vapor concentrations from both instruments agreeing within  $\pm 20\%$ . In addition the following optical particle measurements were used to unambiguously determine the presence of particulate water. The aerosol number density and size distribution from 0.27 to 1550  $\mu\text{m}$  was measured using an FSSP-100 instrument in combination with a Cloud Imaging Probe (CIP). The Multi-wavelength Aerosol Laser Scatterometer (MAS) operates like a backscatter sonde and the Miniature Aerosol Lidar (MAL) measured the profile of aerosol and cloud particles below the aircraft. Backscatter ratios are derived after applying a noise filter, range correction and correction for incomplete overlap in the near range determined from profiles in clear sky. In situ temperature and pressure were measured with a Rosemount probe (TDC) and recorded at 1 Hz. During SCOUT-O3, vertical temperature profiles along the flight track were obtained using the Microwave Temperature Profiler (MTP) [*Denning et al.*, 1989] with a data resolution of about 13 seconds.

### 3. Observations

During the TROCCINOX campaign, ice particles above 380 K have been observed on two out of eight local flights, during SCOUT-O3 on four out of eight. Table 1 lists

the relevant flights and characteristic properties of the atmosphere as observed during these flights. The total time during which ice particles have been encountered in the stratosphere ( $t^{ice}$ ) amounts to about 25 minutes, with about 10 minutes of observations during the flight on 30 November 2005, which included the most extensive probing above the deep convective system “Hector” [Vaughan *et al.*, 2007].

Figure 1 assembles the ice water content observations from all six flights. For better comparison, the basic figure layout is the same as that of Figure 8 b in Kelly *et al.* [1993]. Figure 1 shows volume mixing ratios of particulate water corresponding up to 50 ppmv at 400 K potential temperature and up to 5 ppmv around 415 K. This is considerably higher than the observation of less than 2 ppmv above 400 K by Kelly *et al.* [1993].

Ice-particle-free water vapor observations in the stratospheric overworld are shown in Figure 2. The observed profile depicted in panel (a) is compact, except for several positive deviations. Such positive deviations were present on most flights. In contrast, no prominent negative deviations from the profile have been observed in the stratosphere. Panel (b) shows the distribution of deviations of water vapor ratios for all flights (auxiliary material).

On all flights, the particulate water reported by the water vapor instruments is well correlated with the other particle measurements (Figure 3). Panel (a) depicts the temperature (blue) and potential temperature (red). The static pressure (not shown) was practically constant at 75 hPa. Panel (b) shows that the high water vapor concentrations (blue) due to the presence of ice particles coincide with the particle observations reported by FSSP (red) and elevated backscatter ratios by MAS (green). With relative humidities

between 60 % and 70 % with respect to ice, these particles are in the process of evaporation, but as they are relatively large they may survive for another hour. Finally, panel (c) shows the convective overshoot reaching the aircraft flight level.

#### 4. Hypotheses for observed ice particles

There are three potential explanations for the stratospheric ice particle reported in the previous section: Unintended contrail sampling, in situ formation, or upward transport in convective overshoots with subsequent mixing.

##### 4.1. Unintended contrail sampling

During the TROCCINOX campaign, convective systems were overflown only once, excluding the possibility of measuring the aircraft's own exhaust. Conversely, the flight strategy for several flights during the SCOUT-O3 campaign included circling above deep convective systems, implying some likelihood of such artifacts. We evaluated the possibility of contrail sampling by analyzing the spreading and advection of Geophysica's contrail relative to the aircraft position at later times of the flights (auxiliary material).

Applying this analysis to all flights revealed that during TROCCINOX indeed none of the ice particles observed above 380 K could have originated from the aircraft exhaust. In contrast, during the SCOUT-O3 campaign, about 3 % of the ice particle observations might stem from contrail sampling. These observations are excluded from Figure 1.

## 4.2. In situ formation

Another explanation for the observed ice particles could be in situ nucleation and growth. Adiabatic cooling of air masses lifted above convective systems can lead to supersaturation, inducing the formation of so-called pileus clouds.

We evaluated this hypothesis using a box model simulating the growth and sedimentation of ice particles. For these calculations, relative humidity with respect to ice was fixed to 130%. Results from our calculations are summarized in Figure 4. The figure shows trajectories of growing and falling particles that have nucleated at different altitudes. The colors indicate the time since nucleation. The figure shows that nucleation at 19 km altitude and growth during several hours is needed to explain the observed ice particles with radius of  $30\ \mu\text{m}$  at 17 km. Radar observations during both aircraft campaigns reveal that the convective systems have formed only half an hour prior to the observation of ice particles above 380 K in several cases. It is therefore unrealistic to assume that air above a convective system is lifted substantially for more than an hour. In addition, our observations contradict the assumption of supersaturation at 19 km. Rather, in all observed cases, the ice particles have been embedded in subsaturated air. Finally, CIP reported particle sizes of  $100\ \mu\text{m}$  on several flights during the SCOUT-O3 campaign. Even if there had been 160% relative humidity over ice, such particles would require several hours to grow and would have to have formed deep in the stratosphere above 20 km, because of their high fall speeds. Therefore, the observed ice particles cannot have formed in situ.

### 4.3. Overshooting convection

After having excluded the other two potential explanations, we are left with the third, overshooting convection with subsequent mixing. The most direct evidence for convective overshoots is given by the lidar observations as shown in Figure 3(c), showing the remnants of overshooting convection. Panel (a) shows that the overshooting air has reached similar potential temperature as its surroundings, indicating that it is already well mixed with stratospheric air. A pronounced single peak of lower temperatures ( $\approx 2\text{K}$ ) is found at around 24710s, indicative of limited ongoing overshooting.

We conclude that overshooting convection is the sole possible explanation for the ice particles observed in the stratospheric overworld. As to the effect of these ice particles on the stratospheric water vapor content, it is clear that their evaporation in the sub-saturated air leads to a moistening effect. In fact, the high water vapor mixing ratios reported in Figure 2 (Panel (a)) suggests that there is indeed such a moistening effect. In contrast, there are no indications of “convective dehydration” in the stratosphere, i.e., no anomalously low water vapor mixing ratios were found.

## 5. Conclusion

We have provided clear evidence of convection penetrating the tropical stratosphere. Due to evaporation of the ice particles, the observed events have a hydrating effect on the lower tropical stratosphere. In contrast, no signs of “convective dehydration” could be detected.

A quantitative estimate of the impact of convective overshoots on the stratospheric water vapor content remains a challenge and will require further studies.

**Acknowledgments.** This work was supported by the EU projects TROCCINOX and SCOUT-O3, partly through the Swiss Federal Office for Education and Science. Work performed by MJ Mahoney at the Jet Propulsion Laboratory, California Institute of Technology, was done in part under contract with the National Aeronautics and Space Administration. ECMWF data have been provided by MeteoSwiss.

## References

- Adler, R. F., and R. A. Mack, Thunderstorm cloud top dynamics as inferred from satellite-observations and a cloud top parcel model, *J. Atmos. Sci.*, *43*, 1945–1960, 1986.
- Brewer, A. W., Evidence for a world circulation provided by the measurements of helium and water vapour distribution in the stratosphere, *Q. J. R. Meteorol. Soc.*, *75*, 351–363, 1949.
- Chaboureaud, J. P., J. P. Cammas, J. Duron, P. J. Mascart, N. M. Sitnikov, and H. J. Voessing, A numerical study of tropical cross-tropopause transport by convective overshoots, *Atmos. Chem. Phys.*, *7*, 1731–1740, 2007.
- Corti, T., B. P. Luo, Q. Fu, H. Vomel, and T. Peter, The impact of cirrus clouds on tropical troposphere-to-stratosphere transport, *Atmos. Chem. Phys.*, *6*, 2539–2547, 2006.
- Danielsen, E. F., A dehydration mechanism for the stratosphere, *Geophys. Res. Lett.*, *9*, 605–608, 1982.
- Danielsen, E. F., In situ evidence of rapid, vertical, irreversible transport of lower tropospheric air into the lower tropical stratosphere by convective cloud turrets and by larger-scale upwelling in tropical cyclones, *J. Geophys. Res.-Atmos.*, *98*, 8665–8681, 1993.

- Denning, R. F., S. L. Guidero, G. S. Parks, and B. L. Gary, Instrument description of the airborne microwave temperature profiler, *J. Geophys. Res.-Atmos.*, *94*, 16,757–16,765, 1989.
- Folkins, I., and R. V. Martin, The vertical structure of tropical convection and its impact on the budgets of water vapor and ozone, *J. Atmos. Sci.*, *62*, 1560–1573, 2005.
- Fueglistaler, S., H. Wernli, and T. Peter, Tropical troposphere-to-stratosphere transport inferred from trajectory calculations, *J. Geophys. Res.-Atmos.*, *109*, 2004.
- Holton, J. R., and A. Gettelman, Horizontal transport and the dehydration of the stratosphere, *Geophys. Res. Lett.*, *28*, 2799–2802, 2001.
- Holton, J. R., P. H. Haynes, M. E. McIntyre, A. R. Douglass, R. B. Rood, and L. Pfister, Stratosphere-troposphere exchange, *Rev. Geophys.*, *33*, 403–439, 1995.
- Jensen, E., and L. Pfister, Transport and freeze-drying in the tropical tropopause layer, *J. Geophys. Res.-Atmos.*, *109*, art. no.–D02,207, 2004.
- Kelly, K. K., M. H. Proffitt, K. R. Chan, M. Loewenstein, J. R. Podolske, S. E. Strahan, J. C. Wilson, and D. Kley, Water-vapor and cloud water measurements over darwin during the step 1987 tropical mission, *J. Geophys. Res.-Atmos.*, *98*, 8713–8723, 1993.
- Newell, R. E., and S. Gould-Stewart, A stratospheric fountain, *J. Atmos. Sci.*, *38*, 2789–2796, 1981.
- Nielsen, J. K., N. Larsen, F. Cairo, G. Di Donfrancesco, J. M. Rosen, G. Durrý, G. Held, and J. P. Pommereau, Solid particles in the tropical lowest stratosphere, *Atmos. Chem. Phys.*, *7*, 685–695, 2007.

- Read, W. G., D. L. Wu, J. W. Waters, and H. C. Pumphrey, Dehydration in the tropical tropopause layer: Implications from the uars microwave limb sounder, *J. Geophys. Res.-Atmos.*, *109*, 2004.
- Sherwood, S. C., and A. E. Dessler, A model for transport across the tropical tropopause, *J. Atmos. Sci.*, *58*, 765–779, 2001.
- Sitnikov, N. M., et al., The flash instrument for water vapor measurements on board the high-altitude airplane, *Instruments and Experimental Techniques*, *50*, 113–121, 2007.
- Stefanutti, L., A. R. MacKenzie, S. Balestri, V. Khattatov, G. Fiocco, E. Kyro, and T. Peter, Airborne polar experiment-polar ozone, leewaves, chemistry, and transport (ape-polecat): Rationale, road map and summary of measurements, *J. Geophys. Res.-Atmos.*, *104*, 23,941–23,959, 1999.
- Vaughan, G., C. Schiller, A. R. MacKenzie, K. Bower, T. Peter, H. Schlager, N. R. P. Harris, and P. T. May, Scout-o3 /active: High-altitude aircraft measurements around deep tropical convection, *Bull. Amer. Met. Soc.*, *in Press*, 2007.
- Wang, P. H., P. Minnis, M. P. McCormick, G. S. Kent, and K. M. Skeens, A 6-year climatology of cloud occurrence frequency from stratospheric aerosol and gas experiment ii observations (1985-1990), *J. Geophys. Res.-Atmos.*, *101*, 29,407–29,429, 1996.
- Zoger, M., et al., Fast in situ stratospheric hygrometers: A new family of balloon-borne and airborne lyman alpha photofragment fluorescence hygrometers, *J. Geophys. Res.-Atmos.*, *104*, 1807–1816, 1999.

**Table 1.** List of flights on which ice particles have been observed in the stratospheric overworld (above 380 K potential temperature) during TROCCINOX and SCOUT-O3. Date of flight, mean geometric altitude of 380 K potential temperature ( $z_{380\text{K}}$ ), mean relative humidity over ice between 380 and 400 K potential temperature ( $\overline{RHI}$ ), total ice particle observation period above 380 K ( $t^{ice}$ ), highest geometric altitude ( $z_{max}^{ice}$ ) and potential temperature ( $\theta_{max}^{ice}$ ) of ice particle observation.

Date	$z_{380\text{K}}$	$\overline{RHI}$	$t^{ice}$	$z_{max}^{ice}$ ( $\theta_{max}^{ice}$ )
YYMMDD	km	%	s	km (K)
050204	17.0	66	172	18.0 (410)
050205	17.1	48	12	17.5 (387)
051119	17.8	74	121	18.2 (390)
051125	17.5	54	137	18.9 (415)
051129	17.5	65	477	18.2 (395)
051130	17.4	74	631	18.8 (417)

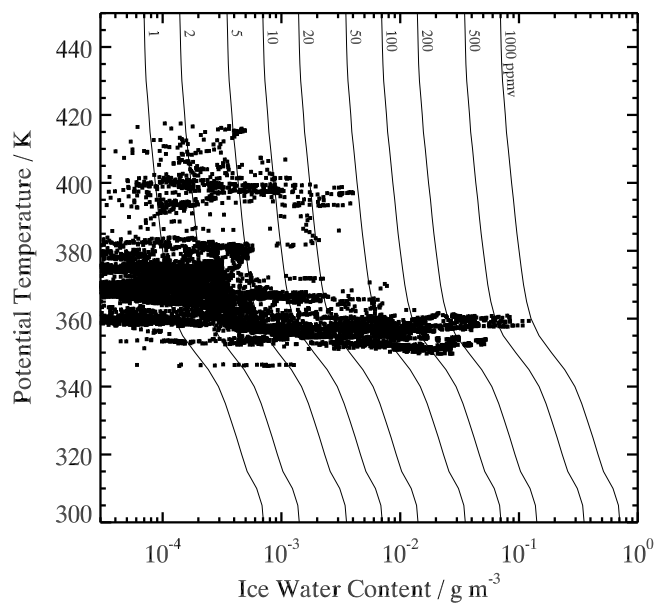


**Figure 1.** Ice water content derived from the measurements by the two water vapor instruments during all six flights listed in Table 1. The contours represent lines of constant volume mixing ratios calculated based on a mean air density profile. Observations suspected to stem from contrail sampling were excluded (see Section 4.1).

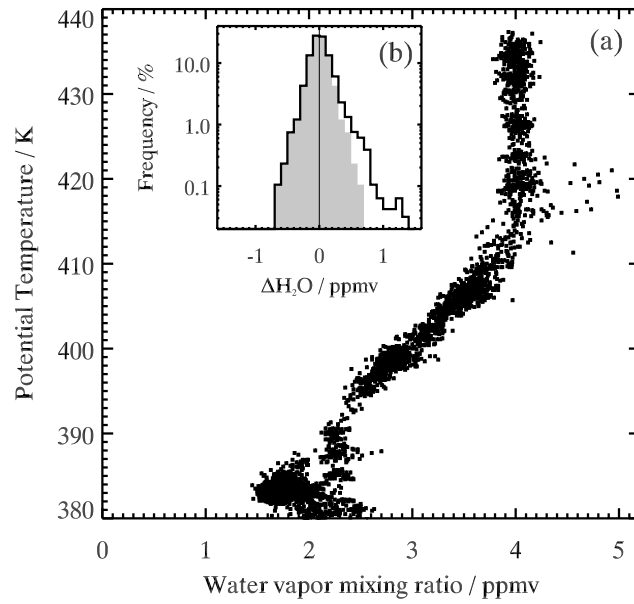


**Figure 2.** Stratospheric water vapor observations in air free of ice particles. (a) Observed vertical profile on 25 November 2005. (b) Probability distribution of water vapor mixing ratio deviations from mean profiles calculated from all flights listed in Table 1. The symmetric gray shading illustrates the distribution's skewness.

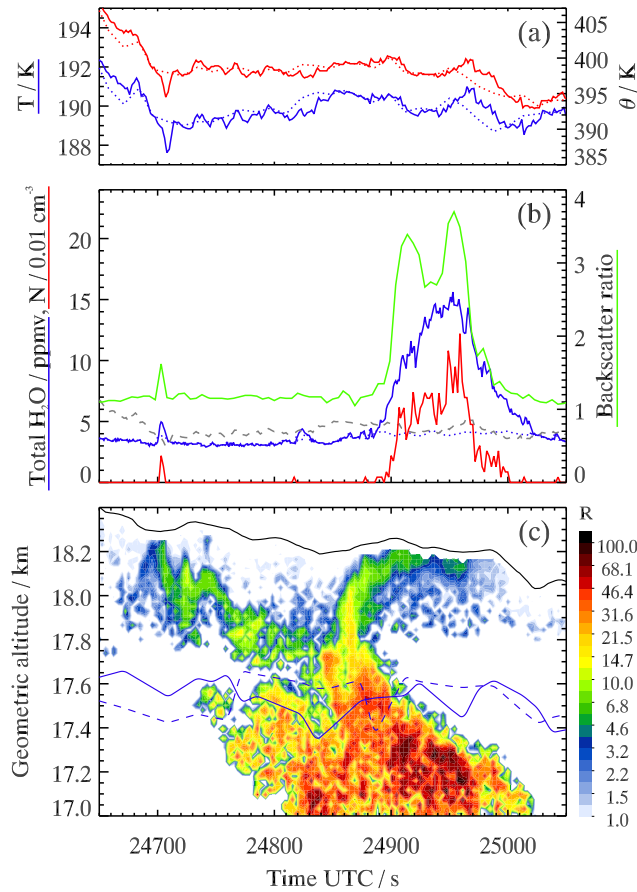


**Figure 3.** Ice particles in the tropical stratosphere observed on 30 November 2005. (a) Temperature (blue) and potential temperature (red) from TDC (solid) and MTP (dotted) at aircraft altitude. (b) Total water (solid blue), gas phase water vapor (dotted blue) and water vapor saturation ratio over ice (dashed gray); FSSP particle number density ( $r > 0.25 \mu\text{m}$ ) (red); MAS total backscatter ratio (green). (c) Backscatter ratio (R) from the downward looking lidar MAL (color-coded). Black curve: aircraft altitude. Blue solid and dashed curves: the 380 K and cold point tropopause, respectively, determined from MTP temperature profiles.

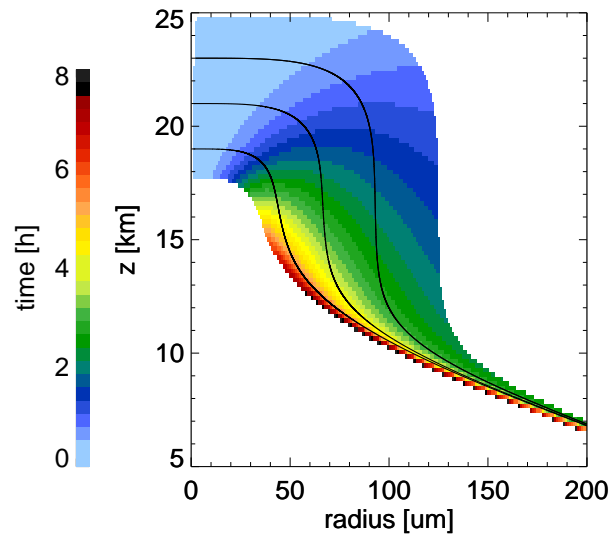


**Figure 4.** Box model results of growth and sedimentation of ice particles at 130 % relative humidity with respect to ice. Trajectories of growing and falling particles (black lines) that have nucleated on different altitudes. The colors indicate the time since nucleation.